Dropwise Condensation on Micro- and Nanostructured Surfaces

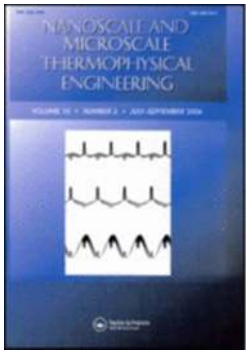

Dropwise Condensation on Micro- and Nanostructured Surfaces

Journal:	*Nanoscale and Microscale Thermophysical Engineering*
Manuscript ID:	UMTE-2013-1232.R1
Manuscript Type:	Special Issue: Micro and Nano Structures for Phase Change Heat Transfer
Date Submitted by the Author:	24-Oct-2013
Complete List of Authors:	Enright, Ryan; Bell Labs Ireland, Alcatel-Lucent Ireland Ltd., Miljkovic, Nenad; Massachusetts Institute of Technology, Alvarado, Jorge; Texas A&M University, Kim, Kwang; University of Nevada, Las Vegas, Rose, John; Queen Mary, University of London,
Keywords:	Surface engineering, Condensation, Phase change

Dropwise Condensation on Micro- and Nanostructured Surfaces

Ryan Enright[1,*], Nenad Miljkovic[2,3], Jorge L. Alvarado[4], Kwang Kim[5] and John W. Rose[6]

[1]*Thermal Management Research Group, Efficient Energy Transfer (ηET) Department, Bell Labs Ireland, Alcatel-Lucent Ireland Ltd., Blanchardstown Business & Technology Park, Snugborough Rd, Dublin 15, Ireland*

[2]*Department of Mechanical Engineering, Massachusetts Institute of Technology, 77 Massachusetts Avenue, Cambridge, Massachusetts 02139, USA*

[3]*Department of Mechanical Science and Engineering, University of Illinois, Urbana, Illinois 61822, USA*

[4]*Department of Engineering Technology and Industrial Distribution and Department of Mechanical Engineering, Texas A&M University, College Station, Texas 77843, USA*

[5]*Department of Engineering, University of Nevada, Las Vegas, 4505 Maryland Parkway, Las Vegas, Nevada 89154, USA*

[6]*School of Engineering and Materials Science, Queen Mary, University of London, London E1 4NS, UK*

Abstract

In this review we cover recent developments in the area of surface-enhanced dropwise condensation against the background of earlier work. The development of fabrication techniques to create surface structures at the micro- and nanoscale using both bottom-up and top-down approaches has led to increased study of complex interfacial phenomena. In the heat transfer community, researchers have been extensively exploring the use of advanced surface structuring techniques to enhance phase-change heat transfer processes. In particular, the field of vapor-to-liquid condensation and especially that of water condensation has experienced a renaissance due to the promise of further optimizing this process at the micro- and nanoscale by exploiting advances in surface engineering developed over the last several decades.

* To whom correspondence should be addressed: ryan.enright@alcatel-lucent.com,

Introduction

Understanding the mechanisms governing water condensation on surfaces is crucial to a wide range of applications that have significant societal and environmental impact, such as energy conversion [1–3], water harvesting [4,5], water desalination [6], thermal management systems [7–11] and environmental control [12]. Water vapor preferentially condenses on solid surfaces rather than directly in the vapor because of the reduced activation energy of heterogeneous nucleation in comparison to homogeneous nucleation [13]. While the excess energy of a surface controls the heterogeneous nucleation process *via* the nucleation rate, it also determines the wetting behavior of the condensate, which has a significant impact on the overall heat and mass transfer performance. Water vapor condensing on high or low surface energy surfaces forms a liquid film or distinct droplets, respectively. The latter, termed dropwise condensation (DWC), is desired since it yields much higher heat transfer coefficients [14,15]. However, high performance dropwise condensers have failed to find widespread application in industry due to the difficulty in identifying a durable low-thermal-resistance DWC promoter for heat transfer materials with characteristically high surface energies [15,16].

The development of fabrication techniques to create surface structures at the micro- and nanoscale using both bottom-up (e.g., chemical oxidation, direct growth) and top-down (e.g., lithography with wet and dry etching) approaches has led to significant growth in the study of complex interfacial phenomena. Advances in surface structuring and functionalization technologies for promoting DWC have allowed researchers to begin exploring the optimization of DWC at the micro- and nanoscales. In this review we first summarize key theoretical and experimental developments in the area of DWC. Next, we detail several important surface functionalization approaches, highlighting some strengths and limitations. We then discuss imaging techniques that are allowing insight into the condensation process at ever decreasing length scales. Finally, we explore several enhanced condensation modes that rely on complex surface modifications at the micro- and nanoscale. For a discussion on internal flow condensation in microchannel geometries we refer the reader to a recent review [17].

Classic dropwise condensation theory & experiment

The theory and mechanism of DWC on smooth surfaces have been well understood for around 50 years [15,18–21]. In a model proposed by Le Fevre and Rose an expression for the heat transfer through a single droplet was combined with an effective mean droplet size distribution to determine the dependence of surface heat flux on vapor-surface temperature difference ΔT [18,19]. Their single droplet heat transfer model considered the conduction resistance, the vapor-liquid interfacial mass transfer, the DWC promoter layer resistance and the effect of interface curvature on the saturation temperature at the droplet surface; which all play significant roles with the relative importance of each depending on droplet size. The droplet surface curvature, along with condensate surface tension and surface subcooling (supersaturation) determines the size of the smallest thermodynamically-viable droplet and hence the number of activated nucleation sites, while the interface mass transfer term is strongly dependent on pressure. The increase in site density causes the heat-transfer coefficient to *increase* with *increasing* vapor-surface temperature difference while the increasing mass transfer resistance causes the heat-transfer coefficient to *decrease* with *decreasing* pressure [15].

Umur and Griffith provided an exact solution for the conduction resistance of a hemispherical droplet by incorporating the interfacial heat transfer coefficient directly into the analysis [22]. This approach avoids the issue of infinite heat transfer at the edge of the droplets obtained by considering the interface and base of the droplet to be at two different temperatures. Also given was an approximation for contact angles other than 90°. Later, Sadhal & Martin developed an expression for the combined conduction and interfacial resistance for arbitrary droplet contact angles between 0° and 90° [23] validated by numerical simulation [24]. Other estimates have been provided for the case of droplets with contact angles greater than 90° [25,26], but did not incorporate a heat transfer coefficient on the droplet interface.

Tanaka used population balance theory to evaluate the local droplet size by taking into account the two mechanisms of growth: direct vapor accommodation onto the droplet and coalescence with neighboring droplets to obtain predictions of the droplet size distribution for small non-coalescing droplets [21]. Since that time, the population balance theory has been used to estimate the population of droplets of a given size [27,28].

Accurate DWC measurements need care to minimize non-condensing gas (NCG) content and prevent build-up of a diffusion boundary layer [15,29,30]. NCG concentrations as little as 3 ppm (μmol/mol) can result in significant error. NCG build-up near the surface as the vapor constituent of the mixture is removed by condensation can result in significantly reduced vapor temperature at the condensing surface. In these circumstances the observed vapor-surface temperature difference is the sum of the temperature drop in the gas-vapor diffusion boundary layer and the required temperature drop across the condensate. Error increases with condensation mass flux and is much more significant for DWC where the condensation mass fluxes are larger and the temperature drop across the condensate is much smaller.

Accurate surface temperature and heat flux measurements are best achieved using flat plate geometries where heat flux and surface temperature can be accurately determined from slope and intercept of temperature distributions in the condenser plate. This geometry is recommended for fundamental condensation measurements and results should be benchmarked against well-documented data sets [30–36]. A set of repeatable data showing the dependence of heat flux on pressure and temperature and comparison with theory is given in Figure 1. It may be noted here that the theory is also in fair agreement with data for ethylene glycol and mercury as well as predicting measurements of dependence of heat-transfer coefficient on maximum droplet size [37]. A general correlation for steam DWC, covering a range of pressures, is given by [15]:

$$\frac{q}{\mathbf{kW/m^2}} = \left(\frac{T}{\mathbf{K}} - 273.15\right)^{0.8}\left[5\frac{\Delta T}{\mathbf{K}} + 0.3\frac{\Delta T^2}{\mathbf{K}}\right], \quad \text{Eq. 1}$$

where q is the heat flux and T is the absolute temperature. Equation Eq**. 1**, which agrees closely with the both experimental data and theory, is recommended as a benchmark for assessing the heat-transfer performance of new promoting techniques on vertical flat plates.

For dropwise condensation on horizontal tubes Eq. 1 might be expected to underestimate the mean heat-transfer coefficient by not more than about 20% [29]. Where tubes have been used it is more convenient to determine the heat flux from mass flow rate and temperatures rise of the coolant, which is accurate to within 2% of temperature gradient measurements to determine heat flux [16,38,39]. Furthermore, tube condensers are more prevalent in industry, making this geometry favorable for practical benchmarking.

Surface functionalization techniques

In order to achieve DWC a functional coating that can impart a reduced surface energy is typically required due to the high surface energy of typical heat transfer materials such as aluminum, copper, titanium and stainless steel. This is a particularly crucial area of DWC research since, in the ~80 years since the discovery of DWC, a satisfactory solution has yet to found that simultaneously satisfies durability, cost and performance requirements. Below we detail several major approaches to realizing suitably low excess surface energies, highlighting their primary strengths and limitations. A summary of these approaches is given in

Table **1**.

Self-assembled monolayers

Self-assembled monolayers (SAMs) rely on the spontaneous formation of a thin molecular film (~1 nm) on the condensing surface comprising individual molecules with hydrophobic tails pointing outwards

from the surface that interacts with the condensate and a ligand that attaches to the condensing surface. This functionalization approach has the advantage that it does not introduce a significant thermal resistance. However, durability remains a primary concern. In early works, SAMs were applied, for example, by immersing copper in a 1% solution of carbon tetrachloride for a period of typically 1 h before rinsing with distilled water. Under laboratory conditions this coating technique gives ideal DWC for some tens of hours before the coating is progressively removed resulting in a steadily decreasing heat transfer coefficient over the course of days [29]. Since this time, a range of SAM molecule options have become available including a number of thiol (sulfur-based ligand) and silane (silicon-based ligand) species with either hydrogenated or fluorinated end groups (tail) that strongly chemisorb with metals/metal oxides and are easy to deposit [41]. In the field of DWC, thiols have been studied more extensively [42,43]. However, the use of silane SAMs in connection with the study of DWC has been on the rise [38,44–51].

In comparison to the silanes, thiols are less stable. Thiols tend to oxidize over short time scales when exposed to the ambient conditions or UV radiation; reducing to disulfides and sulfonates that wash away easily from the surface with polar solvents such as water [4]. Thiols are also less thermally stable than silanes [52]. So while thiols are of use for laboratory studies, they appear to be of limited practical use. On the other hand, silanes are more stable due to covalent bonding with the surface.[41] Furthermore, a range of self-healing strategies have been developed in the recent literature based on fluorinated silane chemistries that could significantly increase the longevity of these coatings[53,54]. Interestingly, there appears to be only limited data available for the longevity of silane-based SAMs during condensation [55].

Polymers

Various polymer coatings have been used to promote DWC including polytetrafluoroethylene (PTFE), parylene and silicones [16,34,56–59]. However, polymer coatings have only proved durable when the layer thickness is such as to effectively offset the advantage of DWC [16]. This limitation may potentially

be overcome using new binder materials to form a stronger bond between the functional polymer and the substrate. Plasma-enhanced vapor deposition of ultra-thin fluoropolymer coatings have been used for fundamental studies of DWC condensation [60]. In addition, initiated chemical vapor deposition of the fluoropolymer thin films is an attractive functionalization method due to high coating conformality and potential robustness [55,61].

Noble metals

It was initially believed that DWC occurred naturally on noble metals [62–64]. However, it was subsequently shown that clean noble metals give film condensation of steam [65]. Thus, DWC may be observed on noble metals due to the presence of physisorbed surface contaminants [66]. Therefore, the barrier for implementing this method of promoting DWC has mainly been limited by the need to replenish surface contaminants to maintain DWC behavior.

Ion implantation

In the mid 1980's Zhang *et al.*[67] and later Qi *et al.*[68] reported that sustained DWC can be achieved through ion implantation of metal surfaces. This early work [69,70] was followed by a series of papers by Leipertz, Froba, Rausch and co-workers which systematically characterized the wettability and durability of ion implanted metal surfaces [71–77]. Carbon, nitrogen, and oxygen ion implantation of copper, aluminum, titanium, and steel surfaces was demonstrated to produce coatings which promoted sustained DWC over periods of multiple months [74]. The mechanism of promotion of DWC involves the formation of nanoscale roughness and chemical heterogeneities produced by particulate precipitates bonded to the metal surfaces [73]. Significant heat transfer improvement is observed on ion implanted surfaces at low subcooling levels, however, the surfaces demonstrate decreasing heat transfer performance when the subcooling level is increased significantly coinciding with the observation of large

irregular droplets and areas undergoing film condensation [73]. Thus far, however, this technique has not yet been utilized in industry primarily due to its high cost.

Rare earth oxides

Recently, Azimi *et al*. provided experimental evidence that rare earth oxides (REOs) are intrinsically hydrophobic and promote DWC of steam [78]. This approach may be potentially advantageous given the toughness of these ceramics compared to SAMs and polymers. However, heat transfer results on these surfaces are not available at this time.

Imaging techniques

Although conventional methods such as optical microscopy are helpful to investigate droplet growth and coalescence [79–81], environmental electron microscopy allows features smaller than a few micrometers to be resolved and includes the techniques of environmental SEM (ESEM) and environmental TEM (ETEM). Generally, ESEM and ETEM have a limited operating pressure range (up to 2.7 kPa) and thus have only been used to image condensation of water near its triple point (273.16 K and 611.73 Pa). The use of ESEM, which allows for imaging of specimens that are "wet," uncoated, or both by allowing gases in the specimen chamber, has been of particular interest for condensation research [82–84]. Figure 2a shows a schematic representation of this imaging technique whereby adjusting the pressure of the water vapor in the specimen chamber and the temperature of the cooling stage, water droplets condense and secondary electrons (SE) are collected to create a high resolution image of the process. Typically, images of droplets (Figure 2b) show strong topographic contrast such that dynamic droplet growth can be observed [44,45,85–89], reliable contact angle measurements can be made and individual droplet heat transfer rates can be calculated [85,90].

During ESEM imaging in the sub-10 μm regime, electron beam heating becomes important [91]. *In situ* ESEM condensation imaging avoiding substrate-related issues can be achieved by removing and

transferring of a small part of the macroscale substrate to a thermally insulated sample platform (Figure 2a) [92]. The perpendicular orientation of the sample with respect to the electron beam limits the absorbed energy and enables simultaneous visualization using secondary (SE - ESEM) and transmitted electrons (TE - STEM) [93]. Figure 2c shows a comparison of ESEM to STEM imaging using the technique, showing higher resolution and smaller beam heating effects. This technique has been used to study different stages of droplet growth on structured surfaces providing insight into the transition of condensing liquid from nano-films forming within the structures, to discrete droplets forming on top of the structure [92].

While ESEM imaging has recently become one of the most utilized condensation imaging methods, other techniques exist which allow for direct imaging beneath condensing droplets to better understand local wetting states. Rykaczewski *et al.* demonstrated a direct method for nano-to-microscale imaging of complex interfaces using cryostabilization [94], cryogenic focused ion beam (FIB) milling, and SEM imaging (cryo-FIB/SEM) (Figure 2d) [95]. This approach has recently been used for imaging of water droplets and frost structures condensed on superhydrophobic (SHS) and lubricant-infused surfaces (LIS) (see schematic layout of the process in Figure 2d) [95,96]. This approach enables identification of individual phases using energy x-ray dispersive spectroscopy (EDS) and also provides quantitative information about interfacial areas between different phases. Other imaging techniques which have been applied to DWC research include infrared imaging and liquid crystal thermography [97–99].

Advanced imaging methods used in combination with quantitative analysis have facilitated understanding of how structure geometry and nucleation density affect the emergent droplet morphology and wetting state. Although these methods provide high spatial resolution (<10 μm), limitations in temporal resolution still make these techniques difficult to use at high heat fluxes when droplet growth dynamics are faster than the image capture speed. Since ESEM software only enables capturing images at rates up to 10 fps, Rykaczewski *et al.* used a screen capture software to capture their results with maximum rate of about 55 fps [100]. Thus, ESEM imaging with rates of several hundreds of frames per

second are achievable and could be even further speed up by balancing obtaining proper contrast through electron beam current and dwell time adjustment (for example 300 ns). The primary roadblock to achieving high speed ESEM is not the hardware, but the ESEM software.

Surface-modified dropwise condensation modes

In this section several different approaches to modifying condensation surfaces are described. A summary of the different approaches is given in

Table **2**.

Superhydrophobic surfaces

Surface-roughness-modified wetting

The use of hydrophobic surfaces with surface roughness/structures smaller than the capillary length scale (Bond number much smaller than unity) has been proposed to enhance condensation heat transfer [9,10,42,43,46,47,91,92,101–105]. Research has focused on using a combination of roughness and low surface energy materials/coatings to create superhydrophobic surfaces, where apparent contact angles exceed 150° and contact angle hysteresis approaches 0° [106,107], for DWC to enhance droplet shedding [26,108–110]. Because wetting interactions can be tuned using structure geometry, these surfaces promise a means to manipulate condensation behavior to realize droplet morphologies ranging from highly pinned, *i.e.*, Wenzel state [111], to superhydrophobic, *i.e.*, Cassie state [112], where droplets can shed passively at microscopic length scales *via* droplet coalescence [42].

Considering a surface with roughness, r, defined by the ratio of the total surface area to the projected area, Wenzel showed when the fluid wets all of the rough area, the *apparent* contact angle θ_W^{app} is defined by [111]:

$$\cos\theta_W^{app} = r\cos\theta\,, \qquad \text{Eq. 2}$$

where θ is Young's angle [113]. Cassie and Baxter considered the case where the droplet rests on the tips of the roughness and showed that the *apparent* contact angle θ_C^{app} is defined by [112]:

$$\cos\theta_C^{app} = \varphi\,(\cos\theta + 1) - 1\,, \qquad \text{Eq. 3}$$

where φ is the ratio of the solid area contacting the droplet to the projected area. The Wenzel state is less desired owing to the higher adhesion typically associated with this wetting state [107]. As a result, many studies have focused on creating and understanding superhydrophobic surfaces to limit droplet adhesion and increase water repellency [106,107,114–117].

In the case of condensation, however, the nucleation of droplets can initiate within the surface roughness and is a *non-equilibrium* wetting process, such that Equations Eq. 2 and Eq. 3, where equilibrium is assumed, may not apply. Previous studies have shown that, on structured superhydrophobic surfaces with well-controlled geometries (Figure 3a), highly adhered Wenzel droplets form during vapor condensation that are distinct from the highly mobile Cassie droplets when deposited using a syringe [102,105,107,118]. In fact, three distinct droplet types are found to exist during condensation; Wenzel (W) (Figures 3a, b), partially wetting (PW) (Figures 3c, d), and Cassie or suspended (S) (Figures 3e, f) droplets. The type of droplet realized is dependent on the surface roughness geometry, nucleation location and nucleation density. Knowledge of the emergent droplet type, contact angle behavior and adhesion needs to be properly characterized and understood in order to tailor the micro/nanostructured surfaces for enhanced heat transfer [38].

Rykaczewski *et al.*[119] and Enright *et al.*[44] demonstrated the relation between droplet growth mode and underlying nanostructure. Specifically, both works showed that confinement of the base area of growing droplet is necessary for formation of high contact angle droplets. Enright *et al.* showed that the morphology of isolated droplets interacting with the surface structures during growth is due to energy

barriers encountered by the droplet growing within the structured surface (Figure 4a) [44]. As a droplet nucleates within the structure and grows to fill the unit cell (volume between structures), it can either grow above the structure forming a 'balloon' like PW droplet (Figure 4b), or laterally spread into the structure forming a highly adhered W droplet (Figure 4c) [44,119]. While the droplet wetting state is dictated by the intricate liquid/structure interaction dynamics, Enright *et al.* showed that it can be conservatively approximated by comparing the energies of the *non-equilibrium* advancing Cassie and Wenzel states with a dimensionless energy ratio:

$$E^* = \frac{\cos\theta_a{}^{CB}}{\cos\theta_a{}^{W}} = \frac{-1}{r\cos\theta_a}. \quad \text{Eq. 4}$$

Equation Eq. 4 implies that, when $E^* > 1$ ($r < -1/\cos\theta_a$), W droplet morphologies are favored, while when $E^* < 1$ ($r > -1/\cos\theta_a$), PW Cassie droplets should emerge [44].

Previous studies have indicated that there must be a surface-structure length-scale dependency, *i.e.*, microstructures [47,101,105] *versus* nanostructures [10,42,43,103,120], suggesting that global thermodynamic analysis, though often used to explain observed condensation behavior [47,101,102,105,119], provides an incomplete description of the dominant wetting state realized during condensation [106]. In addition to the energy criterion (Eq. 4), the nuclei of the droplets need to be separated by 2-5*x* of the spacing between the structures (Figure 4d) ($\langle L\rangle/l > 2{-}5$, where $\langle L\rangle$ is the average spacing between droplets and l is the characteristic spacing of the surface structures). If droplets grow and merge too close to each other ($\langle L\rangle/l < 2{-}5$), the contact line pinning energy barrier associated with individual droplet growth (Eq. 4) is bypassed and flooding of the surface results forming undesired highly adhered W droplets (Figure 4e) [44]. Accordingly, a regime map defining the parametric space with experimentally measured $\langle L\rangle/l$ ratios and calculated E^* in Figure 4f determines the emergent droplet morphology for a wide variety of structure length scales, geometries and nucleation densities. Given this regime map, an important aspect of maintaining nominal DWC behavior becomes being able to define

surface structure spacing, *l*, that is smaller than the separation distances between nucleation centers at a given supersaturation.

Droplet jumping

A key phenomenon associated with condensation on superhydrophobic (low adhesion) surfaces is that when two droplets coalesce, the merged droplet can spontaneously jump away from (normal to) the condensing surface. This phenomenon was first reported in the case of mercury DWC on rough steel surfaces by Kollera and Grigull [121]. The self-propelled motion is powered by the surface energy released upon droplet coalescence [42], and the out-of-plane direction results from the impingement of the liquid bridge between the coalescing droplets on the superhydrophobic substrate [42,122]. The jumping motion has been applied to a variety of phase-change systems [108], including superhydrophobic surfaces that are anti-dew and/or anti-icing [44,49,123–125], enabling the possibility to enhance DWC with nanostructured surfaces [38,43,46,104,126,127].

The self-propelled jumping offers an alternative method for transporting condensate in phase-change systems, independent of any external forces or internal porous wick structures [128]. The autonomous transport can be used to return the condensate in closed-loop systems, such as vapor chambers, in a manner that is fundamentally distinct from the gravity- or capillarity-driven transport [129]. Recently, Miljkovic *et al.* discovered that condensed droplets become charged during the jumping process which opens up the possibility for the control of condensate removal using external electric fields [60]. This may be particularly important for situations where entraining vapor flows begin to dictate the trajectories of jumping droplets resulting in impeded heat transfer [129,130].

Despite considerable interests in the coalescence-induced jumping phenomena, much remains to be understood about the self-propelled jumping process, which is of great practical interest. For example, in designing vapor chambers, the jumping velocity is critical for evaluating the distance the self-propelled droplets can travel [108,129]; in designing superhydrophobic condensers, the threshold radius is crucial

for determining the average size of the condensate droplets [38,42]. Existing models explaining the threshold radius employ an energetic argument assuming a somewhat arbitrary form of viscous dissipation [131–134]. Such models should be further validated with a first-principle model of the complex droplet coalescence process [135]. Future modeling efforts should ideally take into account the surface textures, which introduce additional complexities including moving contact lines, partially wetted cavities, and contact angle hysteresis [136] and asymmetric coalescence [9,127]. These modeling efforts should ideally draw on experimental evidences from both high-resolution electron microscopy and high-speed optical imaging.

Hierarchical superhydrophobic surfaces

Chen and co-workers were the first to report that surfaces with hierarchical nanoscale and microscale topology are superhydrophobic during condensation and promote spontaneous droplet motion [42,43]. Inspiration for such hierarchical architecture comes from nature, for example, the superhydrophobic surface of the lotus leaf [137–141]. Although the mechanism of the two-tier roughness is still not completely understood, Boreyko *et al.* suggested that a mixed Wenzel-Cassie state is possible for the water condensate, where the nano-tier remains dry but the micro-tier is preferentially wetted [142,143]. The role of microscale topology on coalescence dynamics during condensation on hierarchical surfaces been studied theoretically by Liu *et al.* [132,144], Chen *et al.* [10], and Rykaczewski *et al.*[123]. Rykaczewski *et al.*[123] investigated condensation occurring on hierarchical superhydrophobic surfaces consisting of microscale truncated cones with varied dimensions and pitch covered by dense array of nanotrees [10,119,145]. They found that the majority of mobile coalescence events on their hierarchical superhydrophobic surfaces involved the merging of multiple droplets. Their results highlighted the importance of microscale features and provide motivation for further studies of condensation on hierarchical superhydrophobic surfaces with varied microscale topology. In addition, the authors identified that the surface architecture promoting departure of the highest number of microdroplets consisted of microscale features spaced close enough to enable transition of larger droplets into the Cassie

state yet, at the same time, provided sufficient spacing in-between features to allow for mobile coalescence.

Heat transfer on superhydrophobic surfaces

Heat-transfer models for condensation on superhydrophobic surfaces have recently been advanced, being extended from those on smooth DWC surfaces, that deal with the trade-off between droplet mobility (preferring suspended droplets) and thermal conductance (preferring impaled droplets) [45,46,86,108,146,147]. Miljkovic *et al.*[46] and Lee *et al.*[147] extended the Kim model [26], which introduced a conduction resistance term for droplet contact angles greater than 90°, to incorporate geometric details of the structured surface beneath condensing droplets. Furthermore, Miljkovic *et al.* considered the emergent droplet wetting morphology, non-constant contact angle droplet growth and updated the droplet size distribution theory to include both constant and non-constant contact angle droplets growing on surfaces experiencing coalescence-induced droplet jumping [46]. Recently, the feasibility of superhydrophobic nanostructures to enhance DWC has been experimentally demonstrated [38]. Heat transfer enhancements of approximately 30% were achieved on a SAM-functionalized copper oxide-based nanostructured surface relative to a smooth SAM-functionalized surface when the surface was operating in a jumping droplet regime (Figure 5) [38]. However, increasing supersaturation led to flooding of the surface and degraded heat transfer performance. While demonstrated on nanostructured surfaces, the advantage of introducing hierarchically structured surfaces for enhancing condensation heat transfer (besides the condensation area increase that accompanies a hierarchical architecture) remains to be shown. Cheng *et al.* have presented preliminary heat transfer data on a hierarchically-structured surface [126]. However, during heat transfer experiments their surface was flooded and no heat transfer enhancement was observed. Further investigation is needed to understand the role hierarchical structures may play in enhancing heat transfer rates and to develop strategies to prolong the onset of surface flooding to higher supersaturations.

Bi-philic surfaces

It is well known that nucleation on hydrophobic surfaces requires a higher degree of supersaturation than is required when condensing on hydrophilic surfaces [13,148]. Thus, bi-philic surfaces that contain a combination of hydrophilic and hydrophobic regions to reduce the energy barrier for vapor condensation while promoting droplet shedding have been explored in an effort to improve DWC. Kumagai *et al.* were among the first to explore the effects of bi-philic surfaces on condensation heat transfer performance [149]. By patterning their condensing surfaces with alternating stripes of hydrophobic and hydrophilic regions with dimensions at or above the capillary length scale, they showed that heat transfer performance was bounded between the limits of complete DWC and filmwise condensation. More recently, wetting characterization of hybrid surfaces with characteristic length scales below the capillary length has been carried out to study the effects of using alternating hydrophobic and hydrophilic strips [150,151] and hydrophobic/hydrophilic dots on a hydrophilic/hydrophobic background [152] on dynamic droplet contact angles. This understanding is crucial in elucidating the trade-offs between using high-energy condensation sites versus the need to minimize contact angle hysteresis to promote efficient droplet shedding.

Varanasi *et al.*[153] investigated the use of hydrophobic-hydrophilic patterning in combination with structured roughness with the aim of spatially controlling heterogeneous nucleation while facilitating efficient droplet shedding. Using a simple bottom-up deposition process, Mishchenko *et al.*[154] have shown that functionalized hydrophilic polymers and particles deposited on the tips of a range of superhydrophobic structures can induce precise spatial control over water condensation at the micrometer scale. However, results to date indicate that using structured bi-philic surfaces for condensation purposes results in a significant contact angle hysteresis effect due to the hydrophilic tips [155]. Indeed, while the *apparent* advancing angle is independent of the hydrophilic tip wettability, for a fixed structure geometry, increased hysteresis is expected as the local receding contact angle of the hydrophilic tip decreases [152].

He *et al.*[156] developed a unique hierarchically structured superhydrophobic surface comprised of pores with hydrophilic polymer coatings at the base of the pores. Their approach allowed for the efficient condensation of water on the hydrophilic region and surface-tension-driven droplet jumping [142]. They found a significant increase in condensate removal using a bi-philic surface chemistry *versus* a uniformly hydrophobic surface chemistry. Anderson *et al.*[157] studied a unique bi-philic structured surface where the relative placement of the hydrophilic and hydrophobic regions on the surface were reversed compared to previous studies [153,155,158] resulting in hemi-wicking droplets [159]. Their approach relied on Laplace pressure instability to gather droplets independent of coalescence-induced droplet growth mechanics.

Lubricant-infused surfaces

Lubricant-infused surfaces (LIS) consist of micro/nano structures that are functionalized with a low surface energy coating that are subsequently infused with a low surface energy lubricant that is immiscible with the wetting liquid that results in exceptionally low contact angle hysteresis. One of the earliest reports of this phenomenon was in the context of ideal electrowetting surfaces [160], with further description in terms of maximizing droplet mobility [159]. Recently, a range of LIS characteristics were demonstrated based on inspiration from *Nepenthes* pitcher plants [161]. Since then, detailed theoretical descriptions of the phenomenon have been developed [162–164]. LIS are a particularly attractive engineered surface solution because of their omniphobic [161], self-cleaning [162], self-healing [161], and anti-fouling [165] characteristics. Daniel *et al.*[166] demonstrated the promise of LIS to function under elevated temperature conditions where superhydrophobicity tends to fail due to decreasing surface tension. Kim *et al.* studied the wetting behavior of LIS for micro-, nano- and hierchically-structured surfaces [167]. They found that nanostructures alone resulted in the best behavior under high shear conditions in terms of lubricant retention and maintaining low contact angle hysteresis. Anand *et al.* proposed LIS as a viable surface engineering approach to enhance condensation heat transfer based on the observation of water droplet mobility for sizes as small as 100 μm (Figure 6a & b) [168]. Later, Xiao *et*

al.[11] extended the concept of condensation on LIS one step further by introducing a bi-philic functional coating that could increase the nucleation density of droplets due to the reduced interfacial energy between the condensing water and the lubricant; a concept termed "immersion condensation." Combined with the inherent low contact angle and contact angle hysteresis characteristic of LIS, they demonstrated a marked enhancement of ~100% in condensation heat transfer performance *versus* classic DWC in the presence of NCGs (Figure 6c-e).

Conclusions & Future Outlook

The field of DWC has experienced a significant resurgence thanks to new imaging techniques allowing unprecedented access to the growth of droplets on substrates and the proliferation of fabrication techniques that is allowing researchers to realize increasingly sophisticated engineered surfaces. However, as new knowledge is gained it is important that past lessons are also appreciated. Guidelines developed over ~80 years for performing condensation heat transfer measurements should be closely followed including test section design that removes the influence of NCGs. The number of studies demonstrating condensation phenomena on enhanced surfaces greatly exceeds the number of studies quantifying condensation heat transfer performance. This gap needs to close in order for different approaches to be validated. At the very least, high definition imaging experiments should be performed with the aim to provide an expectation of performance before carrying out global heat transfer experiments on large area samples [46]. Long-term condensation studies are needed to validate the durability of new surface structuring and functionalization approaches. Physical failure mechanisms should be identified under both laboratory and industrial conditions and accelerated testing methods should be explored. We stress that maintaining long-term DWC remains the primary barrier to practical implementation for industrial applications. Furthermore, the scalability of surface structuring and functionalization approaches needs to be considered in the context of likely applications.

In superhydrophobic condensation, improved understanding of the droplet jumping process for a range of surface characteristics and condensation conditions is needed. In light of the flooding mechanism that has so far limited enhanced heat transfer rates on superhydrophobic surfaces, strategies including structure scale reduction and control of droplet nucleation density should be explored. From the studies reviewed here, recommendations can be made regarding the feasibility and applicability of superhydrophobic surfaces for enhanced condensation. If the condensation heat flux is relatively low (<8 W/cm^2) the ideal superhydrophobic surface should meet the following 5 criteria if it is to be comparable to or exceed the heat transfer performance of a smooth dropwise condensing surface having low contact angle hysteresis: 1) the partially wetting droplet morphology should be favored, 2) the structure length scale should be minimized (<2 μm), 3) the density of the structures should be high, 4) the thermal conductivity of the structure material should be as high as possible, and 5) the hydrophobic coating covering the structure should be highly conformal and ultra-thin (<40 nm) in order to minimize parasitic thermal resistances. However, if the condensation conditions are such that heat fluxes exceed ≈8 W/cm^2, a smooth dropwise condensing surface with low contact angle hysteresis will have better performance due to nucleation site saturation and flooding of the superhydrophobic surface. Note, the limit of 8 W/cm^2 is the current state-of-the-art superhydrophobic performance. With further reduction of structure length scale (increased structure density), this heat transfer threshold for jumping/flooding should increase and make superhydrophobic surfaces a more viable option for high heat flux applications.

The implementation of bi-philic surface chemistries and roughness at sub-capillary length scales for condensing surfaces is a potentially promising route to enhance condensation rates. The ability to tailor both droplet growth and departure behavior using a range of wetting heterogeneity and structures opens up a large design space for condensing surfaces. However, systematic global heat transfer measurements and detailed heat transfer models for these surfaces are still lacking. Thus, there remains a significant need for studies to demonstrate the efficacy of bi-philic surfaces in condensation heat transfer applications.

While the potential for heat transfer enhancement on LIS has been demonstrated, systematic studies along with further theory development will be required to find the optimum design for these surfaces in the context of heat transfer. A key question regarding LIS is the long-term operability of these surfaces and the impact of progressive lubricant drainage on condensation heat transfer performance. While this issue has yet to be systematically addressed in the context of condensation heat transfer, the results of Kim *et al.* suggest that nanostructured LIS, rather than microstructured or hierarchical LIS, may be the most promising in minimizing lubricant loss [167]. However, the impact of lost lubricant during water droplet shedding remains to be assessed. Furthermore, passively improving condensation performance in the presence of NCG remains an outstanding issue though LIS have shown promise in addressing this issue [11]. However, the mechanism by which LIS improves the performance of DWC in the presence of NCG remains poorly understood.

Finally, while much recent research has focused on the interaction of condensing water with structured surfaces, condensation rate enhancement techniques at the nano- and microscale for low surface tension liquids remains an outstanding problem. In the case of structured, low-energy surfaces, realization of the mobile Cassie state becomes increasingly difficult to achieve as the wetting angle of the condensate reduces. Clever surface designs that spatially-control condensation coupled with structures that can promote a meta-stable Cassie wetting state may offer a solution. However, such an approach will still be limited by the increased nucleation rates expected for low surface tension liquids [13,148]. Here LIS may offer a more feasible solution by maintaining low contact angle hysteresis for droplets with characteristically small contact angles. Thus, heat transfer measurements for such systems should be pursued.

Nomenclature

E^*	Dimensionless energy ratio	-
h_c	Heat transfer coefficient	W/(m^2 K)

q	Heat flux	W/m^2
$<L>$	Mean separation distance between nucleation sites	m
l	Surface structure spacing	m
$\ddot{m}$	Mass flux	kg/(s m^2)
r	Roughness factor	-
T	Temperature	K
γ_{sv}	Solid vapor interfacial energy	J/m^2
γ_{sl}	Solid-liquid interfacial energy	J/m^2
γ_{lv}	Liquid-vapor interfacial energy	J/m^2
θ	Young contact angle	°
θ_a	Advancing contact angle	°
θ_C^{app}	Cassie *apparent* contact angle	°
θ_W^{app}	Wenzel *apparent* contact angle	°

Acknowledgements

The authors would like to thank Prof. Konrad Rykaczewski, Prof. Chuan-Hua Chen and Prof. Kripa Varanasi for valuable discussions. Bell Labs Ireland thanks the Industrial Development Agency (IDA) Ireland for their financial support. N.M. gratefully acknowledges funding support from the MIT S3TEC Center, an Energy Frontier Research Center funded by the Department of Energy, Office of Science, Basic Energy Sciences under Award # DE-FG02-09ER46577.

References

[1] Beér J. M., 2007, "High efficiency electric power generation: The environmental role," Prog. Energy Combust. Sci., **33**(2), pp. 107–134.

[2] Glicksman L. R., and Hunt Jr. A. W., 1972, "Numerical simulation of dropwise condensation," Int. J. Heat Mass Transf., **15**(11), pp. 2251–2269.

[3] Thomas D. H., 2010, Energy efficiency through combined heat and power or cogeneration, Nova Scence Publishers, United States Environmental Protection Agency & Oak Ridge National Laboratory.

[4] Love J. C., Estroff L. A., Kriebel J. K., Nuzzo R. G., and Whitesides G. M., 2005, "Self-Assembled Monolayers of Thiolates on Metals as a Form of Nanotechnology," Chem Rev, **105**(4), pp. 1103–1170.

[5] Andrews H. G., Eccles E. A., Schofield W. C. E., and Badyal J. P. S., 2011, "Three-Dimensional Hierarchical Structures for Fog Harvesting," Langmuir, **27**(7), pp. 3798–3802.

[6] Khawaji A. D., Kutubkhanah I. K., and Wie J. M., 2008, "Advances in seawater desalination technologies," Desalination, **221**(1-3), pp. 47–69.

[7] Miljkovic N., and Wang E. N., 2011, "Modeling and optimization of hybrid solar thermoelectric systems with thermosyphons," Sol. Energy, **85**(11), pp. 2843–2855.

[8] Leach R. N., Stevens F., Langford S. C., and Dickinson J. T., 2006, "Dropwise Condensation: Experiments and Simulations of Nucleation and Growth of Water Drops in a Cooling System," Langmuir, **22**(21), pp. 8864–8872.

[9] Rykaczewski K., Scott J. H. J., Rajauria S., Chinn J., Chinn A. M., and Jones W., 2011, "Three dimensional aspects of droplet coalescence during dropwise condensation on superhydrophobic surfaces," Soft Matter, **7**(19), pp. 8749–8752.

[10] X. Chen J. W., 2011, "Nanograssed micropyramidal architectures for continuous dropwise condensation," Adv Funct Mater, **21**(24), pp. 4617–4623.

[11] Xiao R., Miljkovic N., Enright R., and Wang E. N., 2013, "Immersion Condensation on Oil-Infused Heterogeneous Surfaces for Enhanced Heat Transfer," Sci Rep, **3**(1988).

[12] Pérez-Lomabard L., Ortiz J., and Pout C., 2008, "A review on buildings energy consumption information," Energy Build., **40**(3), pp. 394–398.

[13] Kashchiev D., 2000, Nucleation: Basic Theory with Applications, Butterworth-Heinemann, Oxford.

[14] Schmidt E., Schurig W., and Sellschopp W., 1930, "Versuche über die Kondensation von Wasserdampf in Film- und Tropfenform," Tech. Mech. Thermodyn., **1**(2), pp. 53–63.

[15] Rose J. W., 2002, "Dropwise condensation theory and experiment: A review," Proc. Inst. Mech. Eng. Part J. Power Energy, **216**(2), pp. 115–128.

[16] Marto P. J., Looney D. J., Rose J. W., and Wanniarachchi A. S., 1986, "Evaluation of organic coatings for the promotion of dropwise condensation of steam," Int. J. Heat Mass Transf., **29**(8), pp. 1109–1117.

[17] Kandlikar S. G., Colin S., Peles Y., Garimella S., Pease R. F., Brandner J. J., and Tuckerman D. B., 2013, "Heat Transfer in Microchannels—2012 Status and Research Needs," J. Heat Transf., **135**(9), pp. 091001–091001.

[18] Le Fevre, E. J., and Rose, J. W., 1966, "A theory of heat transfer by dropwise condensation," Proc. Third Int. Heat Transfer Conf., pp. 362–375.

[19] Rose J. W., and Glicksman L. R., 1973, "Dropwise condensation - The distribution of drop sizes," Int J Heat Mass Tran, **16**(2), pp. 411–425.

[20] Rose J. W., 1976, "Further aspects of dropwise condensation theory," Int. J. Heat Mass Transf., **19**(12), pp. 1363–1370.

[21] Tanaka H., 1975, "A Theoretical Study of Dropwise Condensation," J. Heat Transf., **97**(1), pp. 72–78.

[22] Umur A., and Griffith P., 1965, "Mechanism of Dropwise Condensation," J. Heat Transf., **87**(2), pp. 275–282.
[23] Sadhal S. S., and Martin W. W., 1977, "Heat transfer through drop condensate using differential inequalities," Int. J. Heat Mass Transf., **20**(12), pp. 1401–1407.
[24] Ahrendts, A., 1972, "Der Warmeleitwiderstand eines Kondensattropfens," Wärme-Stoffübertragung, **5**, pp. 239–244.
[25] Rose J. W., 1972, "Dropwise condensation of mercury," Int. J. Heat Mass Transf., **15**(7), pp. 1431–1434.
[26] Kim S., and Kim K. J., 2011, "Dropwise condensation modeling suitable for superhydrophobic surfaces," J Heat Transf., **133**(8), pp. 081502–1 – 081502–7.
[27] Wen H. W., and Jer R. M., 1976, "On the heat transfer in dropwise condensation," Chem. Eng. J., **12**(3), pp. 225–231.
[28] Maa J. R., 1978, "Drop size distribution and heat flux of dropwise condensation," Chem. Eng. J., **16**(3), pp. 171–176.
[29] Citakoglu E., and Rose J. W., 1968, "Dropwise condensation—some factors influencing the validity of heat-transfer measurements," Int. J. Heat Mass Transf., **11**(3), pp. 523–537.
[30] Le Fevre E. J., and Rose J. W., 1965, "An experimental study of heat transfer by dropwise condensation," Int. J. Heat Mass Transf., **8**(8), pp. 1117–1133.
[31] Tanner D. W., Pope D., Potter C. J., and West D., 1968, "Heat transfer in dropwise condensation at low steam pressures in the absence and presence of non-condensable gas," Int. J. Heat Mass Transf., **11**(2), pp. 181–190.
[32] Wilmshurst, R., and Rose, J. W., 1970, "Dropwise condensation - further heat transfer measurements," Proc. Fourth Int. Heat Transfer Conf., p. Paper Cs 1–4.
[33] Graham C., 1969, The Limiting Heat Transfer Mechanisms of Dropwise Condensation, Massachusetts Institute of Technology, Department of Mechanical Engineering.
[34] Stylianou S. A., and Rose J. W., 1980, "Dropwise Condensation on Surfaces Having Different Thermal Conductivities," J. Heat Transf., **102**(3), pp. 477–482.
[35] Tanaka H., and Tsuruta T., 1984, "A microscopic study of dropwise condensation," Int. J. Heat Mass Transf., **27**(3), pp. 327–335.
[36] Hatamiya, S., and Tanaka, H., 1986, "A study on the mechanism of dropwise condensation. Part 1: Measurement of heat transfer coefficient of steam at low pressure," Trans Jap Sco Mech Engrs Ser B, **52**(476), pp. 1828 – 1833.
[37] Rose J. W., 1988, "Some aspects of condensation heat transfer theory," Int. Commun. Heat Mass Transf., **15**(4), pp. 449–473.
[38] Miljkovic N., Enright R., Nam Y., Lopez K., Dou N., Sack J., and Wang E. N., 2012, "Jumping-droplet-enhanced condensation on scalable superhydrophobic nanostructured surfaces," Nano Lett, **13**(1), pp. 179–187.
[39] Das A. K., Andeen G. B., Kumar A., Kilty H. P., and Marto P. J., 1999, "The Use of an Organic Self-Assembled Monolayer Coating to Promote Dropwise Condensation of Steam on Horizontal Tubes," J. Heat Transf., **122**(2), pp. 278–286.
[40] Rose, J. W., 1964, "On the mechanism of dropwise condensation," PhD thesis, London University.
[41] Ulman A., 1996, "Formation and Structure of Self-Assembled Monolayers," Chem. Rev., **96**(4), pp. 1533–1554.
[42] Boreyko J. B., and Chen C.-H., 2009, "Self-propelled dropwise condensate on superhydrophobic surfaces," Phys Rev Lett, **103**(18), p. 184501.
[43] Chen C.-H., Cai Q., Tsai C., Chen C.-L., Xiong G., Yu Y., and Ren Z., 2007, "Dropwise condensation on superhydrophobic surfaces with two-tier roughness," Appl Phys Lett, **90**(17), p. 173108.

[44] Enright R., Miljkovic N., Al-Obeidi A., Thompson C. V., and Wang E. N., 2012, "Condensation on superhydrophobic surfaces: The role of local energy barriers and structure length scale," Langmuir, **28**(40), pp. 14424–14432.
[45] Enright R., Miljkovic N., Dou N., Nam Y., and Wang E. N., 2013, "Condensation on superhydrophobic copper oxide nanostructures," J Heat Transf., **135**(9), p. 091304.
[46] Miljkovic N., Enright R., and Wang E. N., 2012, "Effect of droplet morphology on growth dynamics and heat transfer during condensation on superhydrophobic nanostructured surfaces," ACS Nano, **6**(2), pp. 1776–1785.
[47] Wier K. A., and McCarthy T. J., 2006, "Condensation on ultrahydrophobic surfaces and its effect on droplet mobility: ultrahydrophobic surfaces are not always water repellant," Langmuir, **22**(6), pp. 2433–2436.
[48] Feng J., Qin Z., and Yao S., 2012, "Factors affecting the spontaneous motion of condensate drops on superhydrophobic copper surfaces," Langmuir, **28**(14), pp. 6067–6075.
[49] Feng J., Pang Y., Qin Z., Ma R., and Yao S., 2012, "Why condensate drops can spontaneously move away on some superhydrophobic surfaces but can not on others?," ACS Appl Mater Interfaces.
[50] Miljkovic N., Preston D. J., Enright R., Adera S., Nam Y., and Wang E. N., 2013, "Jumping Droplet Dynamics on Scalable Nanostructured Superhydrophobic Surfaces," J. Heat Transf., **135**(8), pp. 080907–080907.
[51] Nenad M., Rong X., Daniel John P., Ryan E., Ian M., and Evelyn N. W., 2013, "Condensation on Hydrophilic, Hydrophobic, Nanostructured Superhydrophobic and Oil-Infused Surfaces," J. Heat Transf., **135**(8), pp. 080906–080906.
[52] Chandekar A., Sengupta S. K., and Whitten J. E., 2010, "Thermal stability of thiol and silane monolayers: A comparative study," Appl. Surf. Sci., **256**(9), pp. 2742–2749.
[53] Xue C.-H., and Ma J.-Z., 2013, "Long-lived superhydrophobic surfaces," J. Mater. Chem., **1**(13), pp. 4146–4161.
[54] Li Y., Li L., and Sun J., 2010, "Bioinspired Self-Healing Superhydrophobic Coatings," Angew. Chem., **122**(35), pp. 6265–6269.
[55] Paxson A. T., Yagüe J. L., Gleason K. K., and Varanasi K. K., 2013, "Stable Dropwise Condensation for Enhancing Heat Transfer via the Initiated Chemical Vapor Deposition (iCVD) of Grafted Polymer Films," Adv. Mater., p. n/a–n/a.
[56] Haraguchi T., Shimada R., Kumagai S., and Takeyama T., 1991, "The effect of polyvinylidene chloride coating thickness on promotion of dropwise steam condensation," Int. J. Heat Mass Transf., **34**(12), pp. 3047–3054.
[57] Depew C. A., and Reisbig R. L., 1964, "Vapor Condensation on a Horizontal Tube Using Teflon to Promote Dropwise Condensation," Ind. Eng. Chem. Process Des. Dev., **3**(4), pp. 365–369.
[58] Holden K. M., Rose J. W., Wanniarachchi A. S., Marto P. J., and Boone D. H., 1987, "The Use of Organic Coatings to Promote Dropwise Condensation of Steam," J. Heat Transf., **109**(3), pp. 768–774.
[59] 1965, "Parylene Coating Promotes Dropwise Condensation on Condenser Tubes," Chem. Eng. News Arch., **43**(42), p. 45.
[60] Miljkovic, N., Preston, D., Enright, R., and Wang, E. N., 2013, "Electrostatic charging of jumping droplets," Nat Commun, **4**, p. 2517.
[61] Gupta M., Kapur V., Pinkerton N. M., and Gleason K. K., 2008, "Initiated chemical vapor deposition (iCVD) of conformal polymeric nanocoatings for the surface modification of high-aspect-ratio pores," Chem Mater, **20**(4), pp. 1646–1651.
[62] Erb R. A., and Thelen E., 1966, Dropwise Condensation Characteristics of Permanent Hydrophobic System, U.S. Government Printing Office.
[63] Erb R., 1973, "Dropwise condensation on gold," Gold Bull., **6**(1), pp. 2–6.
[64] Woodruff D. W., and Westwater J. W., 1979, "Steam condensation on electroplated gold: Effect of plating thickness," Int. J. Heat Mass Transf., **22**(4), pp. 629–632.

[65] Wilkins D. G., Bromley L. A., and Read S. M., 1973, "Dropwise and filmwise condensation of water vapor on gold," AIChE J., **19**(1), pp. 119–123.
[66] Schrader M. E., 1970, "Ultrahigh-vacuum techniques in the measurement of contact angles. II. Water on gold," J. Phys. Chem., **74**(11), pp. 2313–2317.
[67] Zhang, Q., Lin, Z. Q., and Lin, J. F., 1986, "New materials for dropwise condensation," *th Internationl Heat Transfer Conference, ASME, p. 1677.
[68] Qi Z., Dongchang Z., and Jifang L., 1991, "Surface materials with dropwise condensation made by ion implantation technology," Int. J. Heat Mass Transf., **34**(11), pp. 2833–2835.
[69] Ma X., Rose J. W., Xu D., Lin J., and Wang B., 2000, "Advances in dropwise condensation heat transfer: Chinese research," Chem. Eng. J., **78**(2–3), pp. 87–93.
[70] Zhao Q., and Burnside B. M., 1994, "Dropwise condensation of steam on ion implanted condenser surfaces," Heat Recovery Syst. CHP, **14**(5), pp. 525–534.
[71] Bani Kananeh A., Rausch M. H., Fröba A. P., and Leipertz A., 2006, "Experimental study of dropwise condensation on plasma-ion implanted stainless steel tubes," Int. J. Heat Mass Transf., **49**(25–26), pp. 5018–5026.
[72] Kananeh A. B., Rausch M. H., Leipertz A., and Fröba A. P., 2010, "Dropwise Condensation Heat Transfer on Plasma-Ion-Implanted Small Horizontal Tube Bundles," Heat Transf. Eng., **31**(10), pp. 821–828.
[73] Rausch M. H., Leipertz A., and Fröba A. P., 2010, "On the Characteristics of Ion Implanted Metallic Surfaces Inducing Dropwise Condensation of Steam," Langmuir, **26**(8), pp. 5971–5975.
[74] Leipertz A., and Fröba A. P., 2008, "Improvement of Condensation Heat Transfer by Surface Modifications," Heat Transf. Eng., **29**(4), pp. 343–356.
[75] Lukic N., Diezel L. L., Fröba A. P., and Leipertz A., 2010, "Economical aspects of the improvement of a mechanical vapour compression desalination plant by dropwise condensation," Desalination, **264**(1–2), pp. 173–178.
[76] Rausch M. H., Leipertz A., and Fröba A. P., 2010, "Dropwise condensation of steam on ion implanted titanium surfaces," Int. J. Heat Mass Transf., **53**(1–3), pp. 423–430.
[77] Rausch M. H., Fröba A. P., and Leipertz A., 2008, "Dropwise condensation heat transfer on ion implanted aluminum surfaces," Int. J. Heat Mass Transf., **51**(5–6), pp. 1061–1070.
[78] Azimi G., Dhiman R., Kwon H.-M., Paxson A. T., and Varanasi K. K., 2013, "Hydrophobicity of rare-earth oxide ceramics," Nat Mater, **12**(4), pp. 315–320.
[79] Beysens D., 2006, "Dew nucleation and growth," Comptes Rendus Physique, **7**(9–10), pp. 1082–1100.
[80] Beysens D., Steyer A., Guenoun P., Fritter D., and Knobler C. M., 1991, "How does dew form?," Phase Transitions, **31**(1-4), pp. 219–246.
[81] Fritter D., Knobler C. M., and Beysens D. A., 1991, "Experiments and simulations of the growth of droplets on a surface (breath figures)," Phys Rev, **43**(6), pp. 2858–2869.
[82] Stokes D., 2008, Principles and Practice of Variable Pressure: Environmental Scanning Electron Microscopy (VP-ESEM), Wiley.
[83] Stelmashenko N. A., Craven J. P., Donald A. M., Terentjev E. M., and Thiel B. L., 2001, "Topographic contrast of partially wetting water droplets in environmental scanning electron microscopy," J. Microsc., **204**(2), pp. 172–183.
[84] Rossi M. P., Gogotsi Y., and Kornev K. G., 2009, "Deformation of Carbon Nanotubes by Exposure to Water Vapor," Langmuir, **25**(5), pp. 2804–2810.
[85] Miljkovic N., Enright R., and Wang E. N., 2012, "Growth dynamics during dropwise condensation on nanostructured superhydrophobic surfaces," ASME.
[86] Rykaczewski K., 2012, "Microdroplet Growth Mechanism during Water Condensation on Superhydrophobic Surfaces," Langmuir, **28**(20), pp. 7720–7729.
[87] Anand S., and Son S. Y., 2010, "Sub-micrometer dropwise condensation under superheated and rarefied vapor condition," Langmuir, **26**, pp. 17100–17110.

[88] Miljkovic N., Enright R., Maroo S. C., Cho H. J., and Wang E. N., 2011, "Liquid evaporation on superhydrophobic and superhydrophilic nanostructured surfaces," JHT, **133**(080903).
[89] Miljkovic N., Enright R., and Wang E. N., 2012, "Liquid Freezing Dynamics on Hydrophobic and Superhydrophobic Surfaces," J. Heat Transf., **134**(8), pp. 080902–080902.
[90] Jung Y. C., and Bhushan B., 2008, "Wetting behaviour during evaporation and condensation of water microdroplets on superhydrophobic patterned surfaces," J. Microsc., **229**(1), pp. 127–140.
[91] Rykaczewski K., Scott J. H. J., and Fedorov A. G., 2011, "Electron beam heating effects during environmental scanning electron microscopy imaging of water condensation on superhydrophobic surfaces," Appl Phys Lttrs, **98**(9), pp. 093106 – 093106–3.
[92] Rykaczewski K., and Scott J. H. J., 2011, "Methodology for imaging nano-to-microscale water condensation dynamics on complex nanostructures," ACS Nano, **5**(7), pp. 5962–5968.
[93] Barkay Z., 2010, "Wettability study using transmitted electrons in environmental scanning electron microscope," Appl. Phys. Lett., **96**(18), pp. 183109–3.
[94] Wiedemann S., Plettl A., Walther P., and Ziemann P., 2012, "Freeze Fracture Approach to Directly Visualize Wetting Transitions on Nanopatterned Superhydrophobic Silicon Surfaces: More than a Proof of Principle," Langmuir, **29**(3), pp. 913–919.
[95] Rykaczewski K., Landin T., Walker M. L., Scott J. H. J., and Varanasi K. K., 2012, "Direct Imaging of Complex Nano- to Microscale Interfaces Involving Solid, Liquid, and Gas Phases," ACS Nano, **6**(10), pp. 9326–9334.
[96] Rykaczewski K., Anand S., Subramanyam S. B., and Varanasi K. K., 2013, "Mechanism of Frost Formation on Lubricant-Impregnated Surfaces," Langmuir, **29**(17), pp. 5230–5238.
[97] Grooten M. H. M., and van der Geld C. W. M., 2011, "Dropwise condensation from flowing air–steam mixtures: Diffusion resistance assessed by controlled drainage," Int. J. Heat Mass Transf., **54**(21–22), pp. 4507–4517.
[98] Grooten M. H. M., and van der Geld C. W. M., 2012, "Surface property effects on dropwise condensation heat transfer from flowing air-steam mixtures to promote drainage," Int. J. Therm. Sci., **54**(0), pp. 220–229.
[99] Bansal G. D., Khandekar S., and Muralidhar K., 2009, "Measurement of Heat Transfer During Drop-Wise Condensation of Water on Polyethylene," Nanoscale Microscale Thermophys. Eng., **13**(3), pp. 184–201.
[100] Rykaczewski, K., Landin, T., Varanasi, K. K., and Scott, J. H. J., 2012, "Fast Environmental Scanning Electron Microscopy of Nano-to-microscale Fluidic Processes," Symposium SS: Quantitative In situ Electron Microscopy, MRS Fall Meeting, Boston, MA.
[101] Dorrer C., and Rühe J., 2007, "Condensation and wetting transitions on microstructured ultrahydrophobic surfaces," Langmuir, **23**, pp. 3820–3824.
[102] Narhe R. D., and Beysens D. A., 2007, "Growth dynamics of water drops on a square-pattern rough hydrophobic surface," Langmuir, **23**(12), pp. 6486–6489.
[103] Dorrer C., and Rühe J., 2008, "Wetting of silicon nanograss: from superhydrophilic to superhydrophobic surfaces," Adv Mater, **20**(1), pp. 159–163.
[104] Dietz C., Rykaczewski K., Fedorov A. G., and Joshi Y., 2010, "Visualization of droplet departure on a superhydrophobic surface and implications to heat transfer enhancement during dropwise condensation," Appl Phys Lett, **97**(3), pp. 033104 – 033104–3.
[105] Narhe R. D., and Beysens D. A., 2004, "Nucleation and growth on a superhydrophobic grooved surface," Phys Rev Lett, **93**(7), p. 076103.
[106] Quéré D., 2008, "Wetting and Roughness," Annu. Rev. Mater. Res., **38**(1), pp. 71–99.
[107] Lafuma A., and Quere D., 2003, "Superhydrophobic states," Nat. Mater, **2**(7), pp. 457–460.
[108] Miljkovic N., and Wang E. N., 2013, "Condensation heat transfer on superhydrophobic surfaces," MRS Bull., **38**(397).
[109] Dimitrakopoulos P., and Higdon J. J. L., 1999, "On the gravitational displacement of three-dimensional fluid droplets from inclined solid surfaces," J. Fluid Mech., **395**, pp. 181–209.

[110] Kim H.-Y., Lee H. J., and Kang B. H., 2002, "Sliding of Liquid Drops Down an Inclined Solid Surface," J. Colloid Interface Sci., **247**(2), pp. 372–380.
[111] Wenzel R. N., 1936, "Resistance of solid surfaces to wetting by water," Ind Eng Chem, **28**, pp. 988 – 994.
[112] Cassie A. B. D., and Baxter S., 1944, "Wettability of porous surfaces," Trans Faraday Soc, **40**, pp. 546–551.
[113] Young T., 1805, "An essay on the cohesion of fluids," Philos Trans R Soc, **95**, p. 65.
[114] Gao L. C., Fadeev A. Y., and McCarthy T. J., 2008, "Superhydrophobicity and contact-line issues," MRS Bull., **33**(8), pp. 747–751.
[115] Dorrer C., and Rühe J., 2009, "Some thoughts on superhydrophobic wetting," Soft Matter, **5**(1), pp. 51–61.
[116] Roach P., Shirtcliffe N. J., and Newton M. I., 2008, "Progess in superhydrophobic surface development," Soft Matter, **4**(2), pp. 224–240.
[117] Moulinet S., and Bartolo D., 2007, "Life and death of a fakir droplet: Impalement transitions on superhydrophobic surfaces," Eur. Phys. J. E Soft Matter Biol. Phys., **24**(3), pp. 251–260.
[118] Beysens R. D. N. and D. A., 2006, "Water condensation on a super-hydrophobic spike surface," EPL Eur. Lett., **75**(1), p. 98.
[119] Rykaczewski K., Osborn W. A., Chinn J., Walker M. L., Scott J. H. J., Jones W., Hao C., Yao S., and Wang Z., 2012, "How nanorough is rough enough to make a surface superhydrophobic during water condensation?," Soft Matter, **8**, pp. 8786–8794.
[120] Lau K. K. S., Bico J., Teo K. B. K., Chhowalla M., Amaratunga G. A. J., Milne W. I., McKinley G. H., and Gleason K. K., 2003, "Superhydrophobic carbon nanotube forests," Nano Lett, **3**(12), pp. 1701–1705.
[121] Kollera M., and Grigull U., 1969, "Über das Abspringen von Tropfen bei der Kondensation von Quecksilber," Wärme - Stoffübertragung, **2**(1), pp. 31–35.
[122] Boreyko J. B., and Chen C. H., 2010, "Self-propelled jumping drops on superhydrophobic surfaces," Phys Fluids, **22**(091110).
[123] Rykaczewski K., Paxson A. T., Anand S., Chen X., Wang Z., and Varanasi K. K., 2012, "Multimode multidrop serial coalescence effects during condensation on hierarchical superhydrophobic surfaces," Langmuir, **29**(3), pp. 881–891.
[124] Boreyko J. B., and Collier C. P., 2013, "Delayed frost growth on jumping-drop superhydrophobic surfaces," ACS Nano, **7**(2), pp. 1618–1627.
[125] Zhang Q., He M., Chen J., Wang J., Song Y., and Jiang L., 2013, "Anti-icing surfaces based on enhanced self-propelled jumping of condensed water microdroplets," Chem Commun, **49**, pp. 4516–4518.
[126] Cheng J., Vandadi A., and Chen C. L., 2012, "Condensation heat transfer on two-tier superhydrophobic surfaces," Appl Phys Lett, **101**(131909).
[127] He M., Zhou X., Zeng X., Cui D., Zhang Q., Chen J., Li H., Wang J., Cao Z., Song Y., and Jiang L., 2012, "Hierarchically structured porous aluminum surfaces for high-efficient removal of condensed water," Soft Matter, **8**(25), pp. 6680–6683.
[128] Boreyko J. B., Zhao Y., and Chen C. H., 2011, "Planar jumping-drop thermal diodes," Appl Phys Lett, **99**(234105).
[129] Boreyko J. B., and Chen C.-H., 2013, "Vapor chambers with jumping-drop liquid return from superhydrophobic condensers," Int. J. Heat Mass Transf., **61**(0), pp. 409–418.
[130] Miljkovic, N., Preston, D. J., Enright, R., and Wang, E. N., 2013, "Electric-field-enhanced condensation on superhydrophobic nanostructured surfaces," Rev.
[131] Wang F.-C., Yang F., and Zhao Y.-P., 2011, "Size effect on the coalescence-induced self-propelled droplet," APL, **98**(053112).
[132] Liu T. Q., Sun W., Sun X. Y., and Ai H. R., 2012, "Mechanism study of condensed drops jumping on super-hydrophobic surfaces," Colloids Surf, **414**, pp. 366 – 374.

[133] Peng B., Wang S., Lan Z., Xu W., Wen R., and Ma X., 2013, "Analysis of droplet jumping phenomenon with lattice Boltzmann simulation of droplet coalescence," Appl. Phys. Lett., **102**(15), pp. 151601–4.
[134] Lv C., Hao P., Yao Z., Song Y., Zhang X., and He F., 2013, "Condensation and jumping relay of droplets on lotus leaf," Appl. Phys. Lett., **103**(2), pp. 021601–5.
[135] Sprittles J. E., and Shikhmurzaev Y. D., 2012, "Coalescence of liquid drops: Different models versus experiment," Phys Fluids, **24**(122105).
[136] Reyssat M., Richard D., Clanet C., and Quere D., 2010, "Dynamical superhydrophobicity," Faraday Discuss., **146**(0), pp. 19–33.
[137] Cheng Y. T., and Rodak D. E., 2005, "Is the lotus leaf superhydrophobic?," Appl Phys Lett, **86**, p. 144101.
[138] Cheng Y. T., Rodak D. E., Angelopoulos A., and Gacek T., 2005, "Microscopic observations of condensation of water on lotus leaves," Appl Phys Lett, **87**, p. 194112.
[139] Barthlott, W., and Neinhuis, C., 1997, "Purity of the sacred lotus, or escape from contamination in biological surfaces," Planta, **202**, p. 1.
[140] Mockenhaupt B., Ensikat H.-J., Spaeth M., and Barthlott W., 2008, "Superhydrophobicity of biological and technical surfaces under moisture condensation: stability in relation to surface structure," Langmuir, **24**(23), pp. 13591–13597.
[141] Zheng Y., Han D., Zhai J., and Jiang L., 2008, "In situ investigation on dynamic suspending of microdroplet on lotus leaf and gradient of wettable micro- and nanostructure from water condensation," Appl Phys Lett, **92**, p. 084106.
[142] Boreyko J. B., and Chen C.-H., 2009, "Restoring Superhydrophobicity of Lotus Leaves with Vibration-Induced Dewetting," Phys. Rev. Lett., **103**(17), p. 174502.
[143] Boreyko J. B., Baker C. H., Poley C. R., and Chen C.-H., 2011, "Wetting and Dewetting Transitions on Hierarchical Superhydrophobic Surfaces," Langmuir, **27**(12), pp. 7502–7509.
[144] Liu T., Sun W., Sun X., and Ai H., 2010, "Thermodynamic Analysis of the Effect of the Hierarchical Architecture of a Superhydrophobic Surface on a Condensed Drop State," Langmuir, **26**(18), pp. 14835–14841.
[145] Kim C.-H. C. and C.-J., 2006, "Fabrication of a dense array of tall nanostructures over a large sample area with sidewall profile and tip sharpness control," Nanotechnology, **17**(21), p. 5326.
[146] Miljkovic N., Enright R., and Wang E. N., 2013, "Modeling and optimization of condensation heat transfer on micro and nanostructured superhydrophobic surfaces," J Heat Transf., **135**(111004).
[147] Lee S., Yoon H. K., Kim K. J., Kim S., Kennedy M., and Zhang B. J., 2013, "A dropwise condensation model using a nano-scale, pin structured surface," Int. J. Heat Mass Transf., **60**(0), pp. 664–671.
[148] Carey V. P., 2008, Liquid-Vapor Phase-Change Phenomena, Taylor & Francis Group, LLC, New York & Oxen.
[149] Kumagai S., Tanaka S., Katsuda H., and Shimada R., 1991, "On the enhancement of filmwise condensation heat transfer by means of the coexistence with dropwise condensation sections," Exp. Heat Transf., **4**(1), pp. 71–82.
[150] Drelich J., Wilbur J. L., Miller J. D., and Whitesides G. M., 1996, "Contact Angles for Liquid Drops at a Model Heterogeneous Surface Consisting of Alternating and Parallel Hydrophobic/Hydrophilic Strips," Langmuir, **12**(7), pp. 1913–1922.
[151] Morita M., Koga T., Otsuka H., and Takahara A., 2004, "Macroscopic-Wetting Anisotropy on the Line-Patterned Surface of Fluoroalkylsilane Monolayers," Langmuir, **21**(3), pp. 911–918.
[152] Raj R., Enright R., Zhu Y., Adera S., and Wang E. N., 2012, "Unified Model for Contact Angle Hysteresis on Heterogeneous and Superhydrophobic Surfaces," Langmuir, **28**(45), pp. 15777–15788.
[153] Varanasi K. K., Hsu M., Bhate N., Yang W., and Deng T., 2009, "Spatial control in the heterogeneous nucleation of water," Appl. Phys. Lett., **95**(9), pp. 094101–3.

[154] Mishchenko L., Khan M., Aizenberg J., and Hatton B. D., 2013, "Spatial Control of Condensation and Freezing on Superhydrophobic Surfaces with Hydrophilic Patches," Adv. Funct. Mater., **23**(36), pp. 4577–4584.
[155] Yao C. W., Garvin T. P., Alvarado J. L., Jacobi A. M., Jones B. G., and Marsh C. P., 2012, "Droplet contact angle behavior on a hybrid surface with hydrophobic and hydrophilic properties," Appl. Phys. Lett., **101**(11), pp. 111605–5.
[156] He M., Zhang Q., Zeng X., Cui D., Chen J., Li H., Wang J., and Song Y., 2013, "Hierarchical Porous Surface for Efficiently Controlling Microdroplets' Self-Removal," Adv. Mater., **25**(16), pp. 2291–2295.
[157] Anderson D. M., Gupta M. K., Voevodin A. A., Hunter C. N., Putnam S. A., Tsukruk V. V., and Fedorov A. G., 2012, "Using Amphiphilic Nanostructures To Enable Long-Range Ensemble Coalescence and Surface Rejuvenation in Dropwise Condensation," ACS Nano, **6**(4), pp. 3262–3268.
[158] Mishchenko L., Aizenberg J., and Hatton B. D., 2013, "Spatial Control of Condensation and Freezing on Superhydrophobic Surfaces with Hydrophilic Patches," Adv. Funct. Mater.
[159] David Quéré, 2005, "Non-sticking drops," Reports Prog. Phys., **68**(11), p. 2495.
[160] Verheijen H. J. J., and Prins M. W. J., 1999, "Reversible Electrowetting and Trapping of Charge: Model and Experiments," Langmuir, **15**(20), pp. 6616–6620.
[161] Wong T.-S., Kang S. H., Tang S. K. Y., Smythe E. J., Hatton B. D., Grinthal A., and Aizenberg J., 2011, "Bioinspired self-repairing slippery surfaces with pressure-stable omniphobicity," Nature, **477**, pp. 443–447.
[162] Lafuma A., and Quéré D., 2011, "Slippery pre-suffused surfaces," EPL Eur. Lett., **96**(5), p. 56001.
[163] Hejazi V., and Nosonovsky M., 2011, "Wetting Transitions in Two-, Three-, and Four-Phase Systems," Langmuir, **28**(4), pp. 2173–2180.
[164] Smith J. D., Dhiman R., Anand S., Reza-Garduno E., Cohen R. E., McKinley G. H., and Varanasi K. K., 2013, "Droplet mobility on lubricant-impregnated surfaces," Soft Matter, **9**(6), pp. 1772–1780.
[165] Epstein A. K., Wong T.-S., Belisle R. A., Boggs E. M., and Aizenberg J., 2012, "Liquid-infused structured surfaces with exceptional anti-biofouling performance," Proc. Natl. Acad. Sci., **109**(33), pp. 13182–13187.
[166] Daniel D., Mankin M. N., Belisle R. A., Wong T.-S., and Aizenberg J., 2013, "Lubricant-infused micro/nano-structured surfaces with tunable dynamic omniphobicity at high temperatures," Appl. Phys. Lett., **102**(23), pp. 231603–4.
[167] Kim P., Kreder M. J., Alvarenga J., and Aizenberg J., 2013, "Hierarchical or Not? Effect of the Length Scale and Hierarchy of the Surface Roughness on Omniphobicity of Lubricant-Infused Substrates," Nano Lett., **13**(4), pp. 1793–1799.
[168] Anand S., Paxson A. T., Dhiman R., Smith J. D., and Varanasi K. K., 2012, "Enhanced Condensation on Lubricant-Impregnated Nanotextured Surfaces," ACS Nano, **6**(11), pp. 10122–10129.

Figure Captions

Figure 1. Classical condensation heat transfer experiments. (a) Data for dropwise condensation of steam on a copper surface functionalized with dioctadcyl disulphide [32]. Heat flux and vapor-surface temperature difference measurements are shown for various vapor pressures. Different symbols denote data taken on different days. The solid lines are from the theory of Le Fevre and Rose [18]. (b & c) Dropwise condensation of steam at atmospheric pressure on a vertical copper surface functionalized with dioctadecyl disulphide [40]. Scale bars: 20 mm (b) Heat flux, q = 0.4 MW/m^2; subcooling, ΔT = 2 K; condensation mass flux, $\ddot{m}$ = 0.18 kg/m^2 s. (c) Heat flux, q = 1.4 MW/m^2; subcooling, ΔT = 4 K; condensation mass flux $\ddot{m}$ =0.62 kg/m^2 s.

Figure 2. Condensing droplet characterization techniques. (a) Schematic showing the imaging process of water condensation on nanostructured particles using primary (PE), secondary (SE) and transmitted (TE) electron detectors [92]. (b) Constant base droplet growth on a hydrophobic surface imaged using the gaseous secondary electron detector (GSED) at a 90° angle [119]. (c) Series of ESEM images illustrating micro- and nanoscale imaging of water condensation on CuO particles. Top images show GSED detector images, bottom show STEM images [92]. (d) Step-by-step schematic of the cryogenic-focused ion beam (FIB)/SEM method: (i) water condensation on precooled sample, (ii) rapid plunge freezing in liquid nitrogen slush (LN2), (iii) vacuum transfer and in situ conductive metal deposition, and (iv) cryogenic-FIB/SEM milling and imaging [95]. (e) 52° tilt cryogenic-FIB/SEM images of water condensed on a superhydrophobic surface consisting of silicon nanowires coated with a hydrophobic promoter [95]. Adapted with permission from references [92,95] (Copyright 2013, American Chemical Society) and [119] (Copyright 2012, Royal Society of Chemistry).

Figure 3. Condensing droplet contact angle. Time-lapse schematics of (a) Wenzel (W), (b) partially wetting (PW), and (c) suspended (S) droplet morphologies during growth on the structured surface (schematics not to scale). Environmental scanning electron microscopy (ESEM) images of droplets with the (d) W, (e) PW, and (f) S morphologies on a nanostructured surface (h = 6.1 μm, l = 2 μm, d = 300 nm). Reprinted with permission from references [146] (Copyright 2013, American Society of Mechanical Engineers) and [46] (Copyright 2012, American Chemical Society) .

Figure 4. Effect of structure length scale and nucleation density on emergent droplet morphology. (a) Schematic of a droplet growing within the confines of the structures. The liquid can either expand horizontally by filling up more volume between the nanostructures or by increasing its contact angle and forming a droplet [ref. [119]]. Condensed droplet growth observed using ESEM on structured surfaces with (b) Cassie droplets where l = 2 μm and (c) Wenzel droplets where l = 4 μm [ref. [44]]. Scale bar for (b, c) is 60 μm. Condensation behavior on a microstructured surface (l = 4.5 μm, d = 2 μm, h = 5 μm, and E^* = 0.75 ± 0.04) is shown at a fixed location with a scaled coalescence length of (d) $\langle L\rangle/l$ = 3.54 ± 2.43 (PW droplets) and (e) $\langle L\rangle/l$ = 2.04 ± 0.6 (W droplets) [ref. [44]]. Scale bar for (d, e) is 50 μm. (f) Regime map characterizing the dominant wetting behavior observed during condensation with coordinates of $\langle L\rangle/l$ and E^*. Cassie morphologies (red □) emerge at large $\langle L\rangle/l$ and $E^* \lesssim 1$ (shaded region). Wenzel morphologies (blue ○) emerge at low $\langle L\rangle/l$ and/or $E^* \gtrsim 1$ [ref. [44]]. Adapted with permission from references [44] (Copyright 2013, American Chemical Society) and [119] (Copyright 2012, Royal Society of Chemistry).

Figure 5. Experimental and predicted (Eq. 1) condensation heat transfer coefficients during dropwise, and

jumping-droplet condensation on a tube sample (D_{OD} = 6.35 mm, D_{ID} = 3.56 mm, L = 131 mm) for saturated vapor pressures P_v of (a) 2.2 kPa, (b) 2.7 kPa, and (c) 3.3 kPa [38]. Error bars indicate the propagation of error associated with the fluid inlet and outlet temperatures and pressure measurement. The jumping surface error bars are the largest due to the relatively low heat fluxes measured (q < 80 kW/m^2), corresponding to the smaller fluid inlet to outlet temperature difference. The model predictions (lines) were obtained from Eq. 1 and are in good agreement with DWC on the tube.

Figure 6. (a) Concept of condensation on a LIS and (b) an ESEM image of water condensed on a LIS [168]. Water condensation on (c) a dropwise condensing tube surface and (d) a copper-oxide-based LIS tube surface. (e) The overall (vapor to cooling water) heat transfer coefficient for the LIS surface undergoing immersion condensation in the presence of NCG (P_{NCG} = 30 Pa) is compared to the smooth dropwise (c) and flooded superhydrophobic surfaces [11]. Approximately 100% increase in performance is observed for the LIS surface versus the dropwise condensing surface. Note the generally low overall heat transfer coefficients due to the presence of NCGs. Adapted with permission from references [168] (Copyright 2013, American Chemical Society) and [11] (Copyright 2012, Nature Publishing Group).

Table 1. Summary of surface functionalization techniques for DWC.

Table 2. Summary of surface modified condensation modes for DWC.

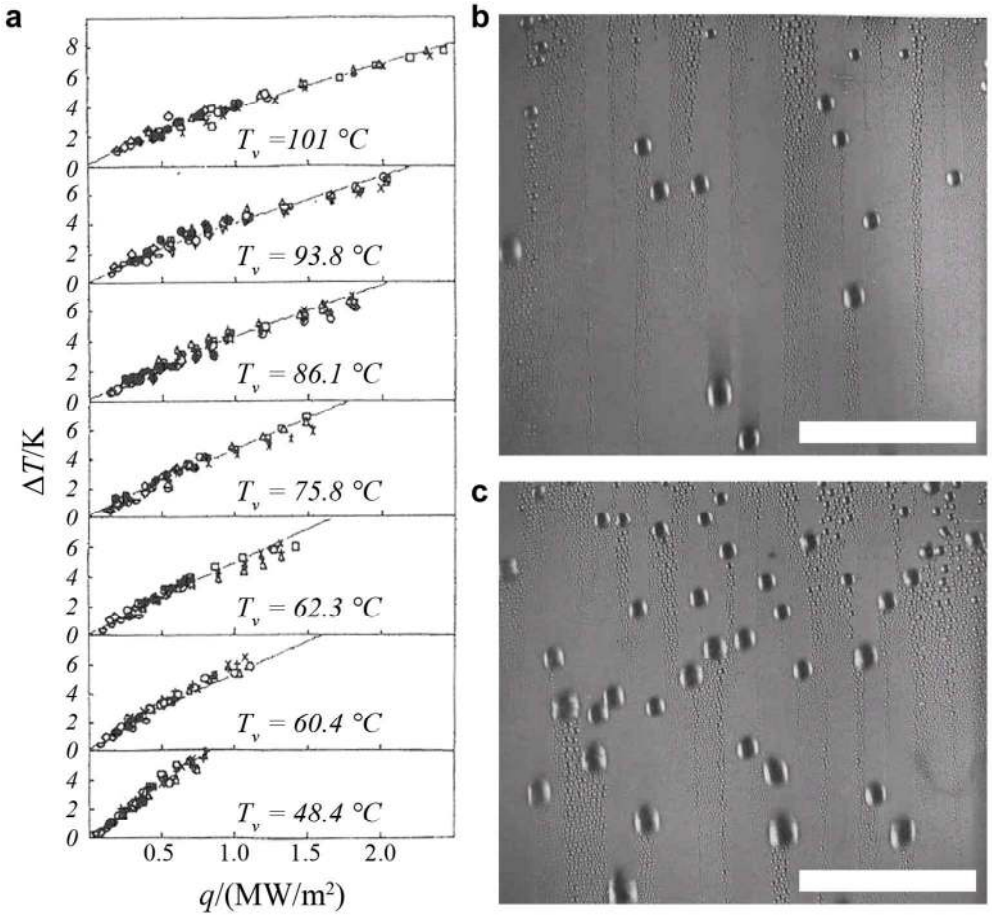

Figure 1
123x113mm (300 x 300 DPI)

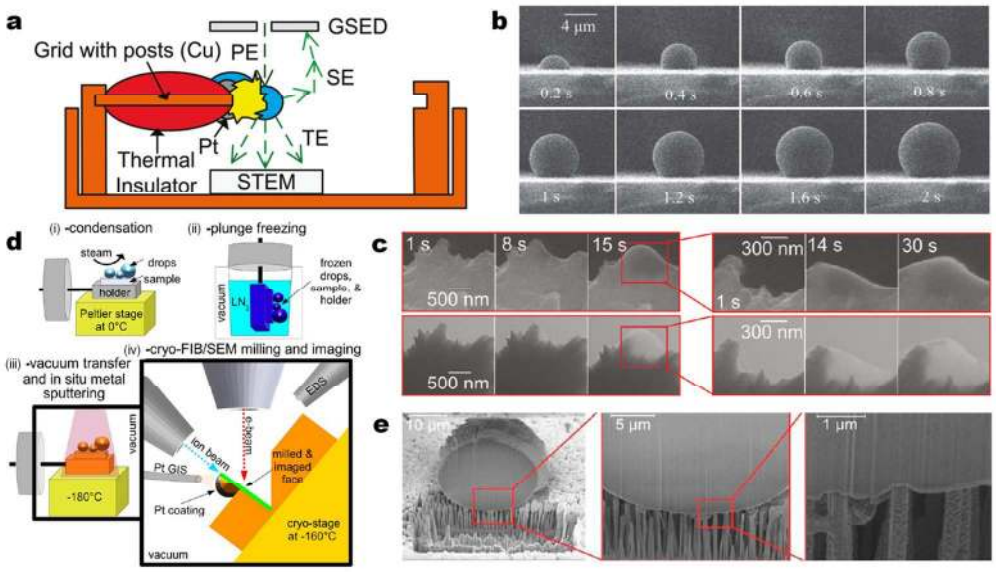

Figure 2
120x70mm (300 x 300 DPI)

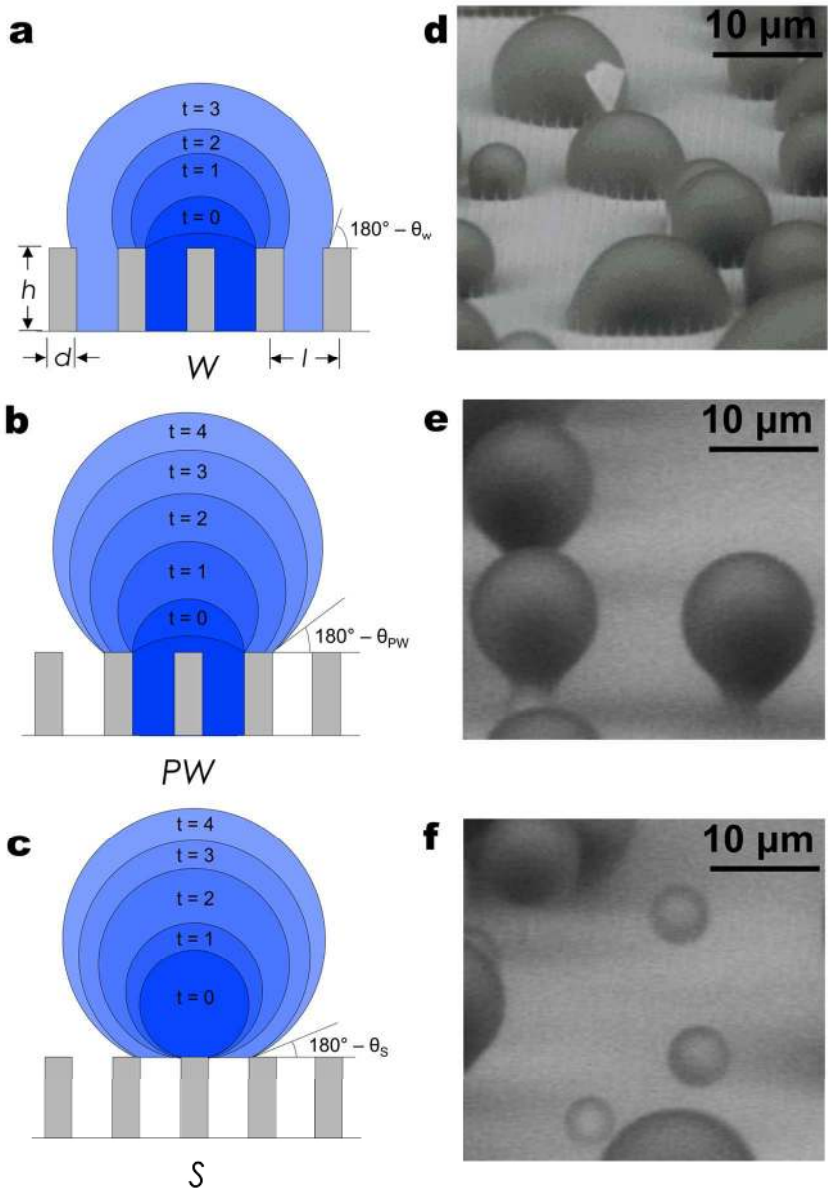

Figure 3
119x171mm (300 x 300 DPI)

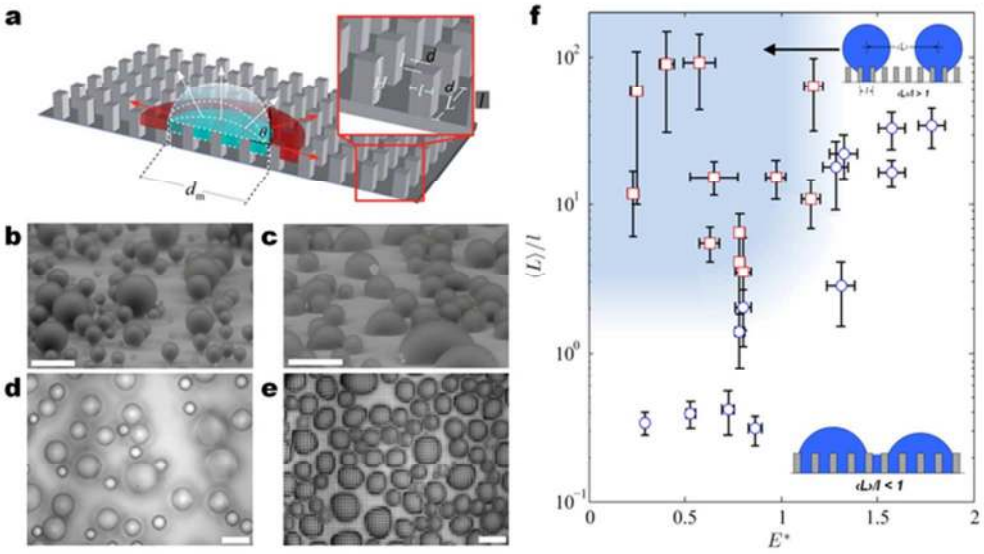

Figure 4
59x33mm (300 x 300 DPI)

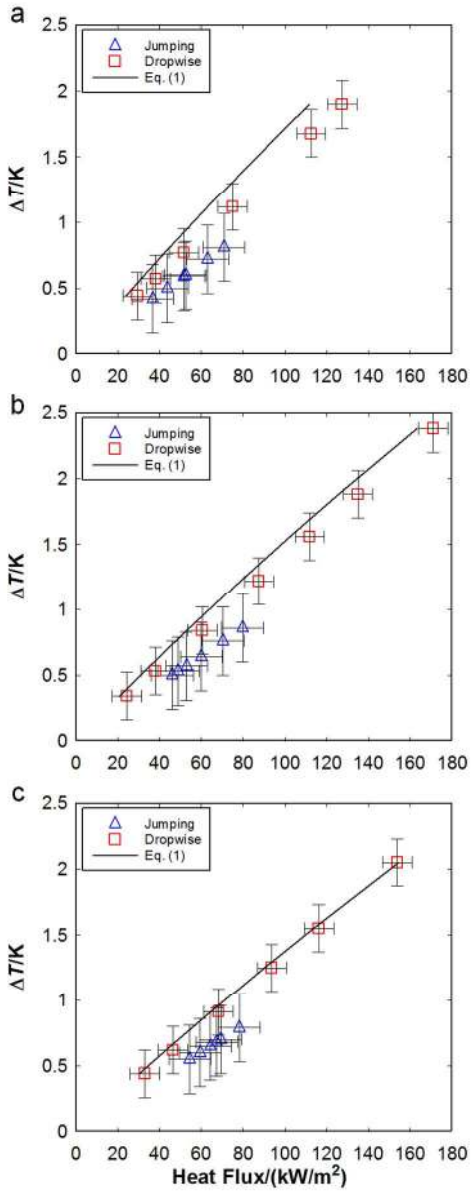

Figure 5
203x515mm (300 x 300 DPI)

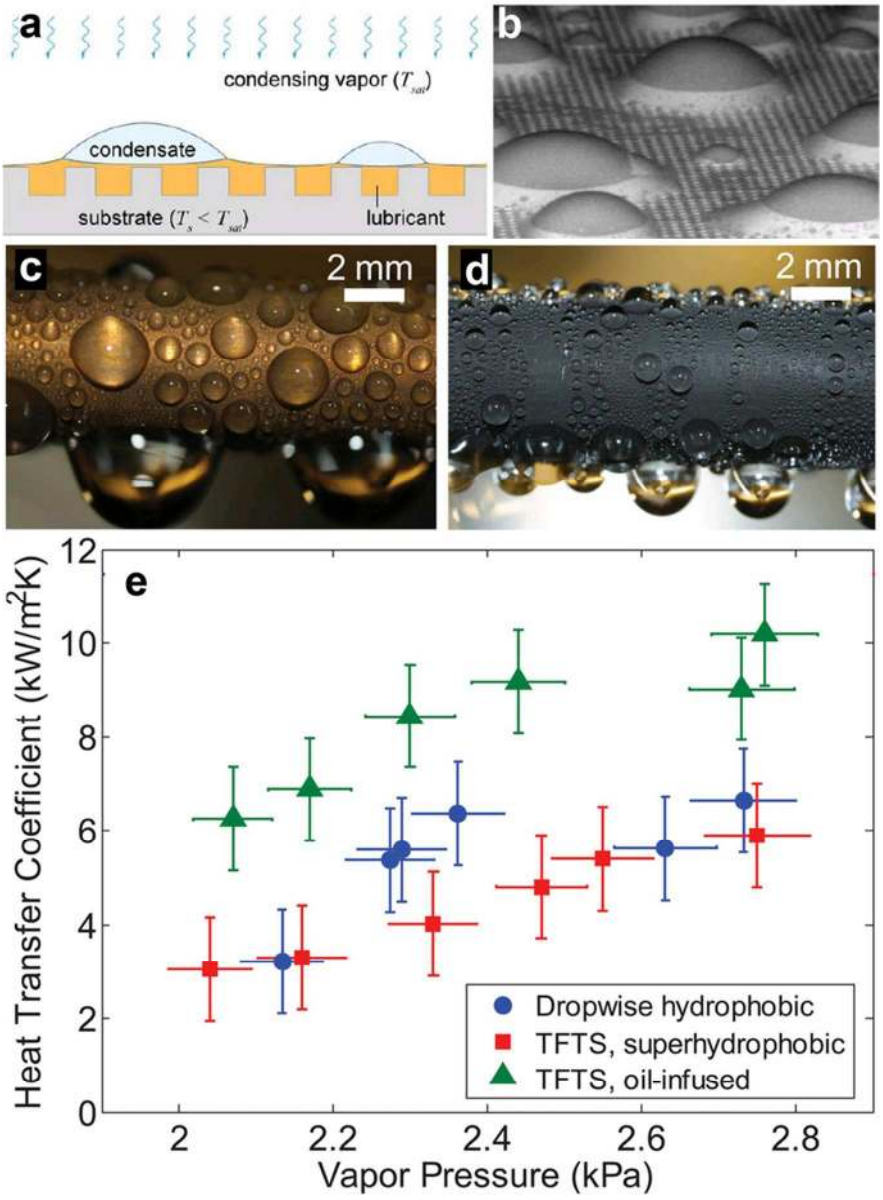

Figure 6
80x109mm (300 x 300 DPI)

Surface Functionalization Technique	Brief Description	Pros	Cons
Self-assembled monolayers (SAMs)	~1-nm thick molecular film on condensing surfaces	Low thermal resistance	Long term durability/stability issues
Polymers	Thin to thick coatings on condensing surfaces	Promote DWC, excellent heat transfer with thin coatings	Robust thin coatings need to be developed
Noble metals (NM)	Applied as a coating on the condensing surface	Promotes DWC if hydrocarbon physiosorbed on surface	Costly, requires contaminant source to maintain DWC
Ion implantation	Carbon, nitrogen and oxygen ions can be implanted on metals	Good heat transfer at low subcooling	Flooding occurs at high subcooling, costly, scalability not demonstrated
Rare earth oxides (REOs)	Ceramic deposited on condensing surface	Intrinsically hydrophobic	Thin coatings required due to low thermal conductivity, heat transfer data not yet available

Table 1
157x120mm (300 x 300 DPI)

Surface-modified Condensation Mode	Brief Description	Pros	Cons
Superhydrophobic surfaces	Surfaces demonstrate high contact angles and low adhesion due to structure enhanced hydrophobicity	Promote droplet jumping to enhance heat transfer rates	Increased thermal resistance of individual droplet growth, surface flooding at high supersaturations
Hierarchical superhydrophobic surfaces	Surfaces consist of micro- and nano-scale features	Promote spontaneous droplet motion, increased condensing surface area	Potential of multiple length scales not yet demonstrated, surface flooding at high supersaturations
Bi-phillic surfaces	Surfaces consist of hydrophobic and hydrophilic regions	Provide spatial control of droplet nucleation	Can exhibit significant contact angle hysteresis; heat transfer data still are lacking.
Lubricant-infused surfaces	Low energy structured surface infused with immiscible low energy liquid	Low hysteresis, low contact angles, nucleation density control	Effects of lubricant drainage still need to be studied

Table 2
157x117mm (300 x 300 DPI)